Atmospheric Chemistry of CH_3CHF_2 (HFC-152a): Kinetics, Mechanisms, and Products of Cl Atom- and OH Radical-Initiated Oxidation in the Presence and Absence of NO_x

Fumikazu Taketani, Tomoki Nakayama, Kenshi Takahashi, and Yutaka Matsumi

Solar-Terrestrial Environment Laboratory and Graduate School of Science, Nagoya University, Honohara 3-13, Toyokawa, Aichi, 442-8507, Japan

Michael D. Hurley and Timothy J. Wallington*

Ford Motor Company, Mail Drop SRL-3083, Dearborn, Michigan 48121

Anne Toft

University of Southern Denmark, Department of Chemistry, Campusvej 55, DK-5230 Odense M, Denmark

M. P. Sulbaek Andersen

Department of Chemistry, University of Copenhagen, Universitetsparken 5, DK-2100 Copenhagen, Denmark

Received: May 2, 2005; In Final Form: July 1, 2005

Smog chamber/Fourier transform infrared (FTIR) and laser-induced fluorescence (LIF) spectroscopic techniques were used to study the atmospheric degradation of CH_3CHF_2. The kinetics and products of the $Cl(^2P_{3/2})$ (denoted Cl) atom- and the OH radical-initiated oxidation of CH_3CHF_2 in 700 Torr of air or N_2; diluents at 295 ± 2 K were studied using smog chamber/FTIR techniques. Relative rate methods were used to measure $k(Cl + CH_3CHF_2) = (2.37 \pm 0.31) \times 10^{-13}$ and $k(OH + CH_3CHF_2) = (3.08 \pm 0.62) \times 10^{-14}$ cm^3 molecule^{-1} s^{-1}. Reaction with Cl atoms gives CH_3CF_2 radicals in a yield of 99.2 ± 0.1% and CH_2CHF_2 radicals in a yield of 0.8 ± 0.1%. Reaction with OH radicals gives CH_3CF_2 radicals in a yield >75% and CH_2CHF_2 radicals in a yield <25%. Absolute rate data for the Cl reaction were measured using quantum-state selective LIF detection of $Cl(^2P_j)$ atoms under pseudo-first-order conditions. The rate constant $k(Cl + CH_3CHF_2)$ was determined to be $(2.54 \pm 0.25) \times 10^{-13}$ cm^3 molecule^{-1} s^{-1} by the LIF technique, in good agreement with the relative rate results. The removal rate of spin−orbit excited-state $Cl^*(^2P_{1/2})$ (denoted Cl*) in collisions with CH_3CHF_2 was determined to be $k(Cl^* + CH_3CHF_2) = (2.21 \pm 0.22) \times 10^{-10}$ cm^3 molecule^{-1} s^{-1}. The atmospheric photooxidation products were examined in the presence and absence of NO_x. In the absence of NO_x, the Cl atom-initiated oxidation of CH_3CHF_2 in air leads to formation of COF_2 in a molar yield of 97 ± 5%. In the presence of NO_x, the observed oxidation products include COF_2 and CH_3COF. As [NO] increases, the yield of COF_2 decreases while the yield of CH_3COF increases, reflecting a competition for CH_3CF_2O radicals. The simplest explanation for the observed dependence of the CH_3COF yield on [NO_x] is that the atmospheric degradation of CH_3CF_2H proceeds via OH radical attack to give CH_3CF_2 radicals which add O_2 to give $CH_3CF_2O_2$ radicals. Reaction of $CH_3CF_2O_2$ radicals with NO gives a substantial fraction of chemically activated alkoxy radicals, $[CH_3CF_2O]^*$. In 1 atm of air, approximately 30% of the alkoxy radicals produced in the $CH_3CF_2O_2$ + NO reaction possess sufficient internal excitation to undergo "prompt" (rate >10^{10} s^{-1}) decomposition to give CH_3 radicals and COF_2. The remaining approximately 70% become thermalized, CH_3CF_2O, and undergo decomposition more slowly at a rate of approximately 2×10^3 s^{-1}. At high concentrations (>50 mTorr), NO_x is an efficient scavenger for CH_3CF_2O radicals leading to the formation of CH_3COF and FNO.

1. Introduction

Recognition of the adverse impact of chlorofluorocarbon (CFC) release into the atmosphere has led to an international effort to replace CFCs with environmentally acceptable alternatives. CH_3CHF_2 (HFC-152a) is currently used as a CFC replacement in foam blowing and aerosol propellant applications. HFC-152a has a short atmospheric lifetime (1.4 years[1]) and a small global warming potential (122 for a 100 year time horizon[1]). Concerns related to global climate change are becoming an increasingly important consideration in the choice of industrial compounds. With its small global warming potential, HFC-152a is becoming a more attractive CFC replacement and may find increased use in high-volume applications currently dominated by HFCs with higher global warming potentials (GWPs), such as in vehicle air-conditioning systems. Prior to large scale use, it is desirable to have a complete understanding of the atmospheric chemistry of HFC-152a.

There have been several previous kinetic studies of the reactions of Cl atoms[2−6] and OH radicals[7−10] with CH_3CHF_2. There are two possible pathways in these reactions:

* Corresponding author. E-mail: twalling@ford.com.

10.1021/jp052270f CCC: $30.25
Published on Web 09/15/2005

$$CH_3CHF_2 + Cl \rightarrow CH_3CF_2 + HCl \quad (1a)$$

$$\rightarrow CH_2CHF_2 + HCl \quad (1b)$$

$$CH_3CHF_2 + OH \rightarrow CH_3CF_2 + H_2O \quad (2a)$$

$$\rightarrow CH_2CHF_2 + H_2O \quad (2b)$$

On the basis of the available experimental studies, the IUPAC subcommittee recommends $k_{1a} = 2.7 \times 10^{-13}$, $k_{1b} = 2.5 \times 10^{-15}$, and $k_2 = k_{2a} + k_{2b} = 3.6 \times 10^{-14}$ cm^3 molecule^{-1} s^{-1} at 298 K.[11] The NASA-JPL panel recommends $k_{1a} = 2.6 \times 10^{-13}$, $k_{1b} = 2.4 \times 10^{-15}$, and $k_2 = k_{2a} + k_{2b} = 3.4 \times 10^{-14}$ cm^3 molecule^{-1} s^{-1} at 298 K.[12] The similarity in the recommendations reflects the mature state of our understanding of the kinetics of reactions 1 and 2.

In contrast to the kinetic database, there have been relatively few studies of the products of the Cl atom- and OH radical-initiated oxidation of CH_3CHF_2. COF_2 has been reported as a product with a molar yield of 0.92−1.0 following Cl atom-initiated oxidation of CH_3CHF_2 in 700−740 Torr of air.[4,6] Reaction of Cl atoms and OH radicals with CH_3CHF_2 can produce either CH_2CHF_2 or CH_3CF_2 radicals. The CH_3CF_2 radical produced in channel 1a or 2a adds O_2 to give a peroxy radical:

$$CH_3CF_2 + O_2 + M \rightarrow CH_3CF_2OO + M \quad (3)$$

The peroxy radical will undergo self-reaction to give the alkoxy radical which is expected to decompose via C−C bond scission.

$$2CH_3CF_2OO \rightarrow 2CH_3CF_2O + O_2 \quad (4)$$

$$CH_3CF_2O + M \rightarrow CH_3 + COF_2 + M \quad (5)$$

The CH_2CHF_2 radical produced in channels 1b and 2b will also add O_2 to give a peroxy radical:

$$CHF_2CH_2 + O_2 + M \rightarrow CHF_2CH_2OO + M \quad (6)$$

The peroxy radical undergoes self-reaction to give the alkoxy radical, which reacts with O_2 to give $CHF_2C(O)H$, which reacts rapidly with OH radicals to generate COF_2.

$$2CHF_2CH_2OO \rightarrow 2CHF_2CH_2O + O_2 \quad (7)$$

$$CHF_2CH_2O + O_2 \rightarrow CHF_2C(O)H + HO_2 \quad (8)$$

$$CHF_2C(O)H + OH + O_2 + M \rightarrow CHF_2C(O)O_2 + H_2O \quad (9)$$

$$2CHF_2C(O)O_2 \rightarrow 2CHF_2C(O)O + O_2 \quad (10)$$

$$CHF_2C(O)O \rightarrow CHF_2 + CO_2 \quad (11)$$

$$CHF_2 + O_2 \rightarrow CHF_2O_2 \quad (12)$$

$$2CHF_2O_2 \rightarrow 2CHF_2O + O_2 \quad (13)$$

$$CHF_2O + O_2 \rightarrow COF_2 + HO_2 \quad (14)$$

Thus, from the COF_2 yield, the oxidation mechanism cannot be made clear.

Under actual atmospheric conditions such as in polluted air masses, the reaction of NO with organic peroxy radicals can proceed efficiently:[13−15]

$$CH_3CF_2OO + NO \rightarrow CH_3CF_2O + NO_2 \quad (15a)$$

$$CH_3CF_2OO + NO + M \rightarrow CH_3CF_2ONO_2 + M \quad (15b)$$

$$CHF_2CH_2OO + NO \rightarrow CHF_2CH_2O + NO_2 \quad (16a)$$

$$CHF_2CH_2OO + NO + M \rightarrow CHF_2CH_2ONO_2 + M \quad (16b)$$

So far, no experimental investigation of the atmospheric degradation of CH_3CHF_2 in the presence of NO has been reported.

In this paper, we report experimental studies on the oxidation processes of CH_3CHF_2 using smog chamber/FTIR techniques and laser-flash photolysis/laser-induced fluorescence techniques. Smog chamber/FTIR experiments were conducted to investigate the Cl- and OH-initiated oxidation of CH_3CHF_2 in 700 Torr of air or N_2 with or without NO. Relative rate methods were used to determine $k_1 = k_{1a} + k_{1b}$ and $k_2 = k_{2a} + k_{2b}$ at 295 ± 2 K. The photooxidation products have been analyzed in detail, and the mechanisms of the photooxidation processes are discussed. Laser-flash photolysis/laser-induced fluorescence experiments were conducted to measure the absolute rate constant of reaction 1. The removal rate constant for spin−orbit excited-state Cl* in collisions with CH_3CHF_2 was determined for the first time.

2. Experimental Section

All experiments (at both Ford and Nagoya) were conducted at 295 ± 2 K. The experimental systems used have been described in detail elsewhere and are described briefly here.

2.1. Smog Chamber/FTIR Apparatus at Ford Motor Company. Experiments were performed in a 140 liter Pyrex reactor interfaced to a Mattson Sirus 100 FTIR spectrometer.[16] The optical path length of the infrared beam was 27 m. The reactor was surrounded by 24 fluorescent blacklamps (GE F15T8-BL) which were used to photochemically initiate the experiments. The Cl($^2P_{3/2}$) (denoted Cl) reaction of CH_3CHF_2 was initiated by UV photolysis of Cl_2 molecules in 700 Torr total pressure of N_2 or air diluent at 295 ± 2 K:

$$Cl_2 + h\nu \rightarrow 2Cl \quad (17)$$

$$CH_3CHF_2 + Cl \rightarrow \text{products} \quad (1)$$

The majority of Cl atoms produced by photolysis of Cl_2 by UV blacklamps will be in the $^2P_{3/2}$ state,[17,18] and any excited Cl atoms will be relaxed efficiently by collisions with the 700 Torr of N_2 or air diluent used in these experiments. Loss of CH_3CHF_2 and formation of products were monitored by FTIR spectroscopy at a resolution of 0.25 cm^{-1}. Infrared spectra were derived from 32 co-added interferograms. All reagents were obtained from commercial sources at purities >99%. In smog chamber experiments, unwanted loss of reactants and products via photolysis, dark chemistry, and wall reactions has to be considered. Control experiments were performed in which CH_3CHF_2/air mixtures, or CH_3CHF_2/Cl_2/air mixtures, were allowed to stand in the chamber in the dark for 1 h and in which CH_3CHF_2/air mixtures were subjected to UV irradiation for 1 h; no loss (<2%) of CH_3CHF_2 was observed.

Smog chamber/FTIR techniques were also employed to study the OH-initiated oxidation of HFC-152a. The reaction of OH radicals with CH_3CHF_2 was initiated by production of OH radicals through UV photolysis of CH_3ONO in the presence of CH_3CHF_2 in 700 Torr total pressure of air diluent.

$$CH_3ONO + h\nu \rightarrow CH_3O + NO \quad (18)$$

$$CH_3O + O_2 \rightarrow CH_2O + HO_2 \quad (19)$$

$$HO_2 + NO \rightarrow OH + NO_2 \quad (20)$$

$$OH + CH_3CHF_2 \rightarrow \text{products} \quad (2)$$

CH_3ONO itself reacts with OH radicals at a modest rate making it difficult to monitor the small loss of less reactive compounds such as CH_3CHF_2. In the present work, we employed a variation on the typical relative rate method in which the loss of CH_3CHF_2 was monitored indirectly by observing the formation of its oxidation product (COF_2). Large initial concentrations of CH_3CHF_2 (0.1 Torr) were used to facilitate monitoring of the COF_2 product resulting from small (<2%) consumptions of CH_3CHF_2. CH_3ONO was prepared by the dropwise addition of concentrated H_2SO_4 to a saturated solution of $NaNO_2$ in methanol and was devoid of any detectable impurities using FTIR analysis. The relative rate method was used to determine the rate constant k_{18} in 700 Torr of air diluent, using C_2H_4 and C_2H_2 as reference gases. C_2H_4 and C_2H_2 have highly structured IR features which are convenient to analyze and react with OH radicals at rates which are well established and so are convenient reference compounds.

Control experiments were performed in which CH_3CHF_2/CH_3ONO/reference compounds/air mixtures were allowed to stand in the chamber in the dark for 1 h and in which CH_3CHF_2/air mixtures were irradiated for 1 h; no loss (<2%) of either CH_3CHF_2 or the reference compounds was observed.

2.2. Vacuum−UV Laser-Induced Fluorescence Spectroscopy System at Nagoya University. The kinetics of reaction 1 were studied using a laser-flash photolysis/laser-induced fluorescence technique.[19] Reactant gases were flowed into the reaction cell which was continuously evacuated by a rotary pump (Alcatel, AC2520). Cl(^2P_j) atoms were generated by the 193 nm photolysis of HCl which produces 59% Cl and 41% Cl*.[20]

$$HCl + h\nu \rightarrow H + Cl \quad (21)$$

$$\rightarrow H + Cl^* \quad (22)$$

The Cl atoms produced from the photodissociation of HCl have relatively little translational excitation because most of the excess energy goes into the translational energy of the H atoms to conserve momentum in the system. Nevertheless, buffer gases were added to the reaction mixtures to suppress hot atom effects. Cl and Cl* atoms were monitored separately using vacuum ultraviolet−LIF (VUV−LIF) at 134.724 nm (4s $^2P_{3/2} \rightarrow$ 3p $^2P_{3/2}$) and 135.166 nm (4s $^2P_{1/2} \rightarrow$ 3p $^2P_{1/2}$). The tunable probe vacuum−UV laser was generated by four-wave mixing ($2\omega_1 - \omega_2$) in Kr gas using two dye lasers pumped by a single XeCl excimer laser (Lambda Physik, COMPex 201, FL3002, and Scanmate 2E).[21] The wavelength of ω_1 was 212.56 nm corresponding to a two-photon resonance to the Kr $5p[1/2]_0$ state. The wavelength of ω_2 was tuned around 500 nm. Typical pulse energies were 0.2 and 4 mJ for 212.56 and 500 nm light, respectively. The ω_1 and ω_2 laser beams were carefully overlapped and focused into a cell containing Kr gas at 15−20 Torr with a fused silica lens ($f = 200$). The resulting vacuum−UV light beam passed through a LiF window into the reaction cell.

The VUV−LIF signal from Cl* or Cl was detected by a solar-blind photomultiplier tube mounted at right angles to the propagation direction of the probing VUV beam and the 193 nm photolysis beam. The 193 nm laser light and the vacuum−UV laser light perpendicularly crossed in the reaction cell. The time delay between the dissociation and probe laser pulses was controlled by a pulse generator (Stanford Research, DG535); the jitter of the delay time was less than 10 ns. Both pump and probe lasers were operated with the repetition rate of 10 Hz. In typical experiments, the delay time was scanned to cover the whole time domain of the fluorescence signal decay, usually $t = 0-900$ μs (with step $\Delta t = 6$ μs) for Cl* and Cl. At each step, the signal was averaged for 10 laser shots and the total time of the decay profile measurement was 150 s.

Two sets of experiments were performed using the LIF technique. First, the rate constant for reaction 1 at 295 ± 2 K was determined from time-resolved LIF detection of Cl. Second, the removal rate constant of Cl* in collisions with CH_3CHF_2 was determined.

The reactivity of ground spin−orbit state Cl atoms toward CH_3CHF_2 was measured by photolysis of HCl/reactant mixtures in 3.0 Torr of CF_4 diluent. Reactant pressures were monitored by a capacitance manometer (Baratron 122A, 10 Torr full scale). CF_4 is an efficient relaxation agent for Cl* atoms with a collisional quenching rate constant of $(2.3-2.4) \times 10^{-11}$ cm^3 molecule^{-1} s^{-1}.[19,22] In the presence of 3.0 Torr of CF_4, the Cl*($^2P_{1/2}$) atoms are relaxed to the ground spin−orbit state within 1 μs. After relaxation of >90% of the Cl* atoms, the subsequent decay of Cl atoms was monitored and used to derive kinetic data for reactions of Cl with CH_3CHF_2.

To investigate the removal rate of Cl* in collisions with CH_3CHF_2, the temporal profiles of Cl* atoms were monitored following the photolysis of HCl/reactant mixtures in 1.5 Torr of Ar diluent. Ar is an inefficient relaxation agent for Cl*($^2P_{1/2}$) atoms (quenching rate constant = $(3 \pm 1) \times 10^{-16}$ cm^3 molecule^{-1} s^{-1} [23]). In all experiments, the concentration of added reactants was at least 1500 times greater than the initial Cl and Cl* atom concentrations and the loss of Cl atoms is expected to follow pseudo-first-order kinetics.

Reagents diluted in buffer gas were introduced into the reaction cell using mass flow controllers (STEC, SEC-400MARK3). The gases used in the experiments had the following stated purities: HCl, 99.9%; CH_3CHF_2, 99.994%; CF_4, 99.99%; and Ar, 99.999%. All gases were used as received without further purification.

3. Results and Discussion

3.1. Relative Rate Study of the Reaction of Cl Atoms with CH_3CHF_2. The kinetics of reaction 1 were measured relative to reactions 23 and 24:

$$CH_3CHF_2 + Cl \rightarrow \text{products} \quad (1)$$

$$CH_4 + Cl \rightarrow \text{products} \quad (23)$$

$$CH_3Cl + Cl \rightarrow \text{products} \quad (24)$$

Reactant mixtures consisted of 7−8 mTorr of CH_3CHF_2, 90−110 mTorr of Cl_2, and 7.5 mTorr of CH_4 or 22.1 mTorr of CH_3Cl in 700 Torr of N_2 or air diluent. The rate constant k_1 was determined by observing the relative loss rates of CH_3CHF_2 and the reference compounds; results are shown in Figure 1. Linear least-squares analysis of the data in Figure 1 gives $k_1/k_{23} = 2.39 \pm 0.15$ and $k_1/k_{24} = 0.49 \pm 0.01$. Using the values of $k_{23} = 1.0 \times 10^{-13}$ [12] and $k_{24} = 4.8 \times 10^{-13}$,[12] we obtain $k_1 = (2.39 \pm 0.15) \times 10^{-13}$ and $(2.35 \pm 0.05) \times 10^{-13}$ cm^3 molecule^{-1} s^{-1}, respectively. We estimate that potential systematic errors associated with uncertainties in the reference rate

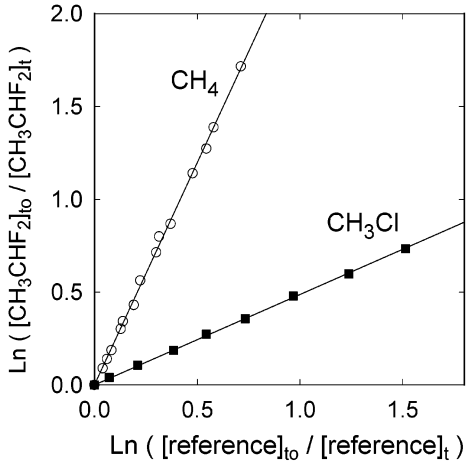

Figure 1. Loss of CH_3CHF_2 vs CH_4 (open circles) and CH_3Cl (filled squares) following exposure to Cl atoms in 700 Torr of N_2 at 295 K.

constants could add an additional 10% to the uncertainty range for k_1. Propagating this additional uncertainty gives $k_1 = (2.39 \pm 0.29) \times 10^{-13}$ and $(2.35 \pm 0.23) \times 10^{-13}$ cm^3 molecule^{-1} s^{-1}. We choose to cite a final value of k_1 which is an average of those determined using the two different reference compounds together with error limits which encompass the extremes of the individual determinations; hence, $k_1 = (2.37 \pm 0.31) \times 10^{-13}$ cm^3 molecule^{-1} s^{-1}. The k_1 value determined in the present study is consistent with the IUPAC[11] and NASA-JPL[12] recommendations discussed in the Introduction.

3.2. Mechanism of the Cl + CH_3CHF_2 Reaction. To establish the relative importance of channels 1a and 1b, experiments were performed using $CH_3CHF_2/Cl_2/N_2$ mixtures. The UV irradiation of such mixtures leads to chain photochemical chlorination of CH_3CHF_2 to give CH_3CF_2Cl and CH_2ClCHF_2 in yields which reflect the relative importance of channels 1a and 1b. For example, the following reactions produce CH_3CF_2Cl:

$$Cl_2 + h\nu \rightarrow 2Cl \tag{17}$$

$$CH_3CHF_2 + Cl \rightarrow CH_3CF_2 + HCl \tag{1a}$$

$$CH_3CF_2 + Cl_2 \rightarrow CH_3CF_2Cl + Cl \tag{25}$$

The potential for loss of CH_3CF_2Cl and CH_2ClCHF_2 via reaction with Cl atoms in such experiments needs to be considered. The rate constant for reaction of Cl atoms with CH_3CF_2Cl is approximately 600 times smaller than k_1.[11] For the consumptions of HFC-152a used in these experiments (10−90%), loss of CH_3CF_2Cl will be negligible. There are no available kinetic data for the reaction of Cl atoms with CH_2ClCHF_2. Hence, we employed relative rate methods similar to those described in section 3.1 to measure k_{26}:

$$Cl + CH_2ClCHF_2 \rightarrow \text{products} \tag{26}$$

With CD_2H_2 and CH_3Cl as reference compounds, we measured $k_{26}/k(Cl + CD_2H_2) = 1.35 \pm 0.11$ and $k_{26}/k(Cl + CH_3Cl) = 0.124 \pm 0.009$. Using values of $k(Cl + CD_2H_2) = 4.57 \times 10^{-14}$ [24] and $k(Cl + CH_3Cl) = 4.8 \times 10^{-13}$,[12] we obtained $k(Cl + CH_2ClCHF_2) = (6.17 \pm 0.50) \times 10^{-14}$ and $(5.95 \pm 0.43) \times 10^{-14}$ cm^3 molecule^{-1} s^{-1}, respectively. Taking an average of the individual determinations, we arrived at $k(Cl + CH_2ClCHF_2) = (6.06 \pm 0.61) \times 10^{-14}$ cm^3 molecule^{-1} s^{-1}. Chlorine atoms are approximately 4 times less reactive toward CH_2ClCHF_2 than toward the parent compound CH_3CHF_2. Hence, in experiments involving irradiation of $CH_3CHF_2/Cl_2/N_2$ mixtures, the CH_2ClCHF_2 product should increase linearly with CH_3CHF_2 for low consumptions (10−20%) of CH_3CHF_2 but for larger consumptions there should be a discernible curvature in the CH_2ClCHF_2 yield plot.

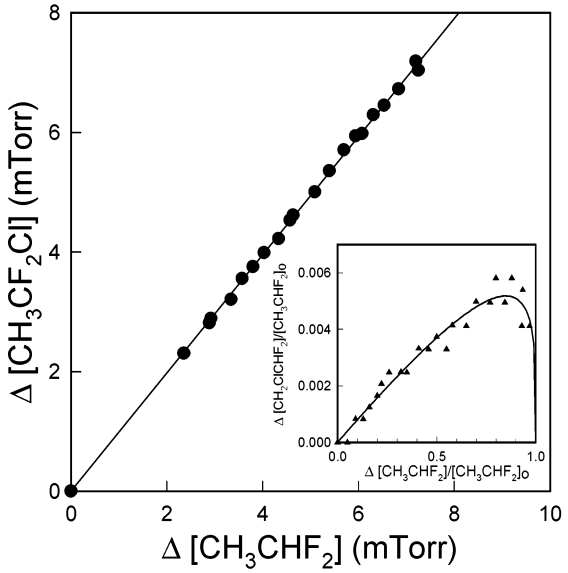

Figure 2. Formation of CH_3CF_2Cl (circles) and CH_2ClCHF_2 (triangles) vs loss of CH_3CHF_2 following UV irradiation of $CH_3CHF_2/Cl_2/N_2$ mixtures. The initial CH_3CHF_2 concentrations in experiments used to determine the CH_3CF_2Cl and CH_2ClCHF_2 yields were 7.6 and 67−133 mTorr, respectively. The line through the CH_3CF_2Cl data is a linear-squares fit, and the curve through the CH_2ClCHF_2 data is a fit to the expression discussed by Meagher et al.[25]

Figure 2 shows a plot of the observed formation of CH_3CF_2Cl and CH_2ClCHF_2 vs loss of CH_3CHF_2 following UV irradiation of $CH_3CHF_2/Cl_2/N_2$ mixtures. As expected, the concentration of CH_3CF_2Cl increases linearly with loss of CH_3CHF_2 and the concentration of CH_2ClCHF_2 increases approximately linearly for modest (<30%) consumptions of CH_3CHF_2, plateaus for consumptions of approximately 80%, and decreases thereafter. Linear least-squares analysis of the CH_3CF_2Cl data gives a yield of 99 ± 4%. The curve in the inset in Figure 2 is a fit of the expression describing the formation and loss of a reactive primary product (CH_2ClCHF_2 in this case) described elsewhere.[25] The best fit shown in Figure 2 was obtained using $k_{26}/k_1 = 0.235 \pm 0.068$ and a CH_2ClCHF_2 yield of 0.81 ± 0.07%. The value of k_{26}/k_1 derived from the observed behavior of the CH_2ClCHF_2 product is entirely consistent with the ratio of the independent determinations reported in section 3.1 and earlier in this section: $k_{26}/k_1 = 0.256 \pm 0.043$. The CH_2ClCHF_2 yield provides a measurement of $k_{1b}/(k_{1a} + k_{1b}) = 0.0081 \pm 0.0007$ and hence, by inference, $k_{1a}/(k_{1a} + k_{1b}) = 0.9919 \pm 0.0007$. These results can be compared to those from the previous investigation by Yano and Tschuikow-Roux.[3] Evaluation of the Arrhenius expression for k_{1a}/k_{1b} reported by Yano and Tschuikow-Roux[3] at 295 K gives values of $k_{1b}/(k_{1a} + k_{1b}) = 0.0086$ and $k_{1a}/(k_{1a} + k_{1b}) = 0.9914$ which are in excellent agreement with those from the present work.

3.3. Absolute Rate Determination for the Reaction of Cl with CH_3CHF_2 Using the VUV−LIF Technique. Figure 3 shows the observed temporal profiles of the two spin−orbit states following the 193 nm pulsed irradiation of a mixture of 14 mTorr of HCl and 620 mTorr of CH_3CHF_2 in 3 Torr of CF_4 diluent. The vertical scale in Figure 3 is the observed fluorescence intensity at 134.724 and 135.166 nm from Cl and Cl*, respectively, in arbitrary units. The time-resolved VUV−LIF

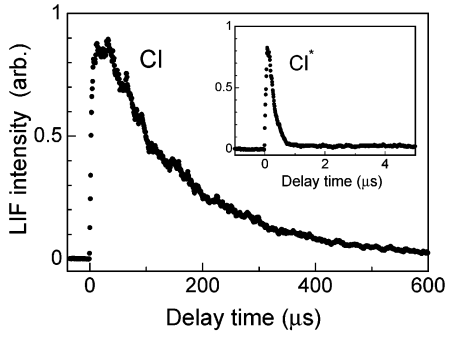

Figure 3. Temporal decay of Cl following flash photolysis of a mixture containing 14 mTorr of HCl and 620 mTorr of CH_3CHF_2 in 3.0 Torr of CF_4 at 295 K. The inset shows the temporal decay of Cl* obtained under the same partial pressure conditions. The Cl and Cl* atom fragments were detected by the VUV−LIF spectroscopy technique at 134.724 and 135.166 nm, respectively.

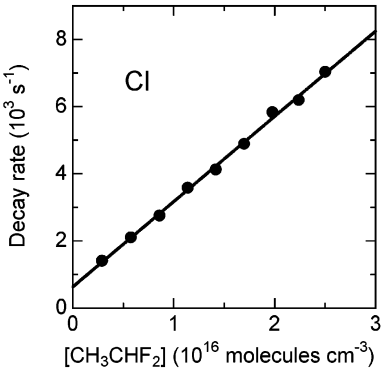

Figure 4. Pseudo-first-order loss of Cl atoms vs CH_3CHF_2 concentration. The line is a linear least-squares fit through the data.

signal of Cl* and Cl atoms produced by the photolysis of HCl exhibits an initial jump followed by a slower decay. The presence of CF_4 diluent relaxes the Cl* atoms into Cl atoms within 1 μs. The subsequent decay of Cl atoms follows pseudo-first-order kinetics and provides information on the kinetics of the Cl + CH_3CHF_2 reaction.

Figure 4 shows a plot of the observed pseudo-first-order decay of Cl atoms in the presence of the CH_3CHF_2 reactant. The line through the data is a linear least-squares fit which gives $k_1 = (2.54 \pm 0.25) \times 10^{-13}$ cm^3 molecule^{-1} s^{-1}. Quoted uncertainties include two standard deviations from the least-squares fits and systematic uncertainties (e.g., precision of concentration measurements). This is the first absolute rate study of the reaction of Cl with CH_3CHF_2. The k_1 value obtained using the VUV−LIF technique agrees with that obtained using the relative rate method described in section 3.1 and with the IUPAC and NASA-JPL recommendations.

3.4. Removal of Cl* Atoms in Collisions with CH_3CHF_2. The temporal decay of the VUV−LIF signal of Cl* following the pulsed laser photolysis of HCl/CH_3CHF_2/Ar mixtures provides a measure of the rate at which Cl* atoms are removed (via physical quenching and chemical reaction) in collisions with CH_3CHF_2. In all experiments, the decay of Cl* atoms followed first-order kinetics. Figure 5 shows a plot of the observed pseudo-first-order loss rates of Cl* vs the concentration of CH_3CHF_2. As seen in Figure 5, the rate of Cl* decay increased linearly with the CH_3CHF_2 concentration. Linear least-squares analysis of the data in Figure 5 gives a rate constant for Cl* loss of $(2.21 \pm 0.22) \times 10^{-10}$ cm^3 molecule^{-1} s^{-1}.

Hitsuda et al.[19] have reported removal rates of Cl* in collisions with C_2H_6, C_2D_6, CH_3F, C_2H_5F, and CH_3CF_3 using

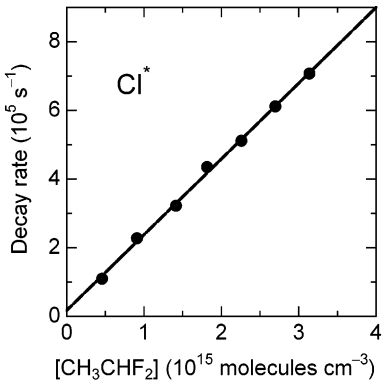

Figure 5. Pseudo-first-order loss of Cl* atoms vs CH_3CHF_2 concentration. The line is a linear least-squares fit through the data.

the VUV−LIF technique. As expected on the basis of similar molecular structure, the removal rate constant of Cl* with CH_3CHF_2 determined in this work, $(2.21 \pm 0.22) \times 10^{-10}$ cm^3 molecule^{-1} s^{-1}, is comparable to that of Cl* with C_2H_5F and CH_3CF_3. Recent studies of the reactive scattering of Cl* with hydrocarbons such as CH_4, CD_4, C_2H_6, C_2D_6, C_3H_8, *n*-C_4H_{10}, and *i*-C_4H_{10} have shown that physical quenching of Cl* to Cl dominates reactive scattering of Cl* to yield HCl and hydrocarbon radicals.[26−29] It seems likely that physical quenching is also the dominant loss mechanism of Cl* in collisions with CH_3CHF_2.

3.5. Product Study of Cl-Initiated Oxidation of CH_3CHF_2 in Air. To investigate the products of the Cl-initiated degradation of CH_3CHF_2 in air (in the absence of NO_x), experiments were performed in which mixtures of 7.6−19.0 mTorr CH_3CHF_2 and 98.6 mTorr Cl_2 in 700 Torr of air diluent were introduced into the reaction chamber and subjected to UV irradiation. Figure 6 shows typical spectra acquired before (A) and after (B) a 2 min irradiation of a mixture containing 7.6 mTorr CH_3CHF_2 and 98.6 mTorr Cl_2 in 700 Torr of air. Comparison of panel B with reference spectra of COF_2 and CO shows the formation of these species. CO formation is explained by the oxidation of CH_3 radicals produced in reaction 5. CH_3 radicals combine with O_2 to give CH_3O_2 radicals which undergo self-reaction leading to the formation of HCHO and CH_3OH. These products are more than 200 times more reactive than CH_3CHF toward Cl atoms. Reaction of Cl atoms with HCHO and CH_3OH leads to the formation of CO.

Figure 7 shows a plot of COF_2 formation vs CH_3CHF_2 loss following UV irradiation of CH_3CHF_2/Cl_2/air mixtures. Linear least-squares analysis gives a molar COF_2 yield of 97 ± 5%. Within experimental uncertainties, the Cl atom-initiated oxidation of CH_3CHF_2 in air leads to essentially 100% molar conversion of CH_3CHF_2 into COF_2. This observation is consistent with the previous reports of Edney and Driscoll[4] and Tuazon and Atkinson.[6] As discussed in section 3.2, Cl atoms react with CH_3CHF_2 to give CH_3CF_2 radicals in a yield of 99.19%. In 700 Torr of air, the sole fate of CH_3CF_2 radicals will be the addition of O_2 to give $CH_3CF_2O_2$ radicals. Observation of COF_2 in a yield of essentially 100% indicates that the fate of $CH_3CF_2O_2$ radicals is self-reaction to give CH_3CF_2O radicals which then decompose via C−C bond scission to give CH_3 radicals and COF_2.

3.6. Product Study of Cl-Initiated Oxidation of CH_3CHF_2 in the Presence of NO. To study the products of Cl atom-initiated oxidation of CH_3CHF_2 in air in the presence of NO_x, reagent mixtures consisting of 7.5−8.6 mTorr of CH_3CHF_2, 220−261 mTorr of Cl_2, and 11−143 mTorr of NO in 700 Torr

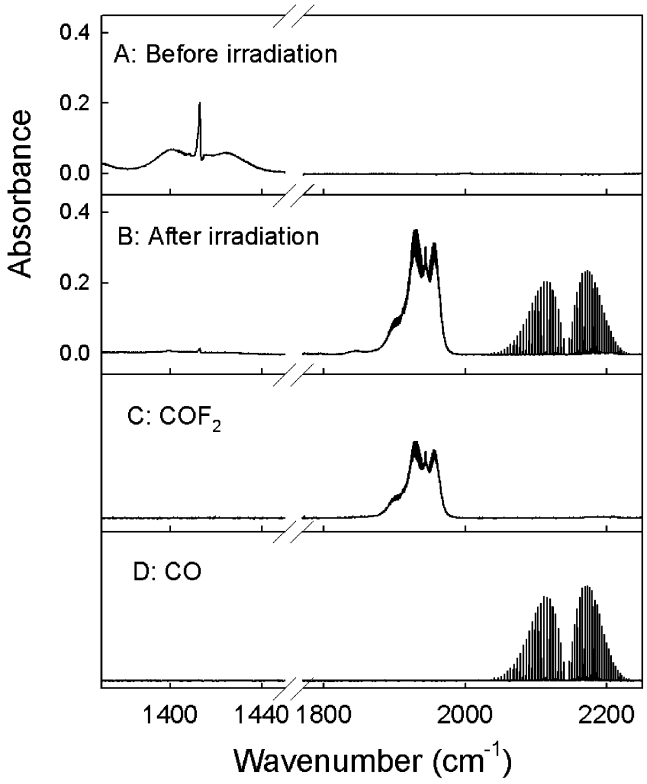

Figure 6. 1370−1450 and 1770−2250 cm^{-1} portions of infrared spectra obtained (A) before and (B) after a 2 min irradiation of mixture containing 7.6 mTorr of CH_3CHF_2 and 98.6 mTorr of Cl_2 in 700 Torr of air at 295 K. Panels C and D show reference spectra of COF_2 and CO.

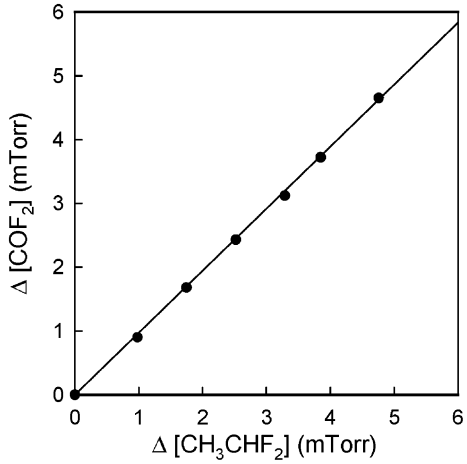

Figure 7. Formation of COF_2 vs loss of CH_3CHF_2 following UV irradiation of CH_3CHF_2/Cl_2/air mixtures.

of N_2/O_2 diluent were introduced into the reaction chamber and subjected to UV irradiation. Figure 8 shows typical spectra acquired before (A) and after (B) a 55 min irradiation of a mixture containing 7.5 mTorr of CH_3CHF_2, 261 mTorr of Cl_2, and 143 mTorr of NO in 700 Torr of air. Panel C shows the result of subtracting NO features from spectrum B. Comparison of panel C with the reference spectra of ClNO, CH_3COF, and COF_2, panels D−F, shows the formation of these species.

Experiments were performed with the initial NO concentration varied over the range 11−143 mTorr. As shown in Figure 9, the yield of CH_3COF increased at the expense of that of COF_2 as the NO concentration was increased from 10 to 60 mTorr. However, for experiments employing concentrations of NO greater than 60 mTorr, there was little discernible effect from

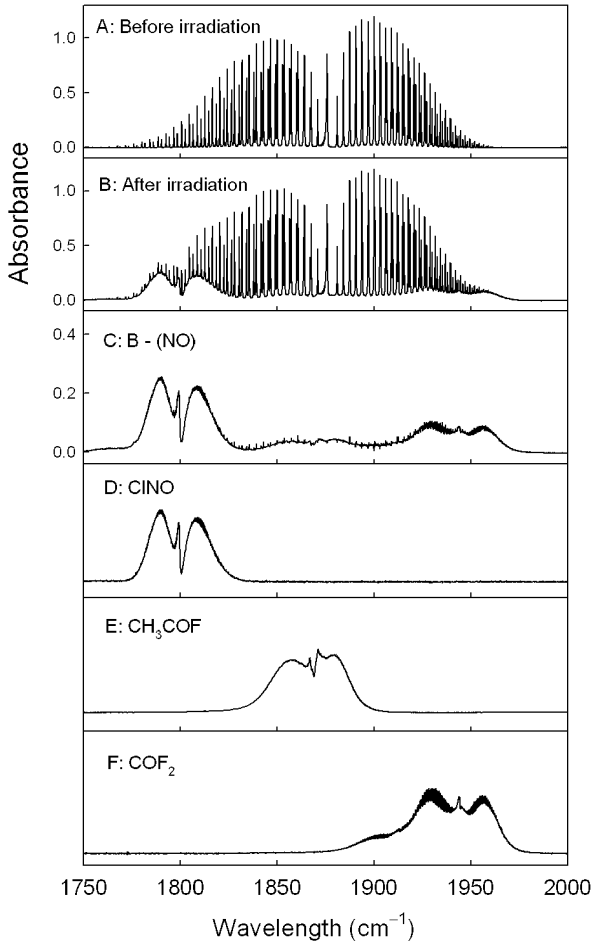

Figure 8. Infrared spectra acquired (A) before and (B) after a 55 min irradiation of a mixture containing 7.5 mTorr of CH_3CHF_2, 261 mTorr of Cl_2, and 143 mTorr of NO in 700 Torr of air at 295 K. Panel C is the result of subtracting NO features from panel B. Panels D−F show reference spectra of ClNO, CH_3COF, and COF_2.

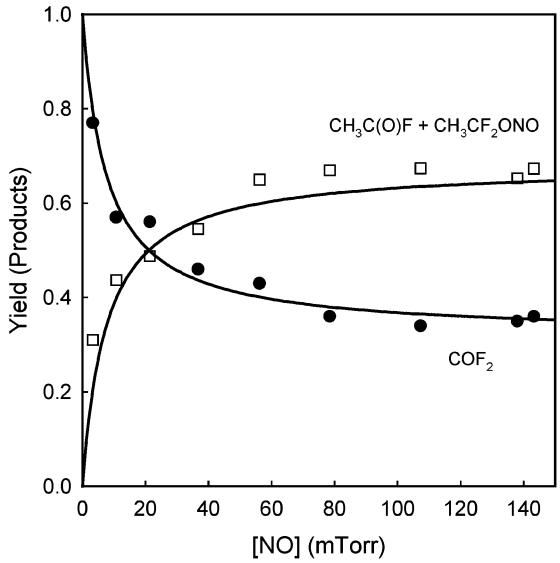

Figure 9. Molar yield of COF_2 (circles) and $CH_3COF + CH_3CF_2$-ONO (squares) observed following the UV irradiation of mixtures of 8 mTorr of CH_3CHF_2, 240 mTorr of Cl_2, and 11−143 mTorr of NO in 700 Torr of air at 295 K. The curves are fits of expression I to the data; see text for details.

the NO concentration. The simplest sequence of reactions that explains the behavior in Figure 9 is:

$$CH_3CF_2OO + NO \rightarrow CH_3CF_2O + NO_2 \quad (15a)$$

$$CH_3CF_2OO + NO \rightarrow CH_3CF_2O^* + NO_2 \quad (15c)$$

$$CH_3CF_2O^* \rightarrow CH_3 + COF_2 \quad (27)$$

$$CH_3CF_2O \rightarrow CH_3 + COF_2 \quad (5)$$

$$CH_3CF_2O + NO \rightarrow CH_3COF + FNO \quad (28)$$

The reaction of peroxy radicals (e.g., CH_3CF_2OO) with NO proceeds via two channels giving alkoxy radicals and NO_2 as dominant products and organic nitrates as minor products. The nitrate yield in the reaction of halogenated peroxy radicals with NO is sufficiently small such that it can be neglected in the present analysis. A significant fraction of the alkoxy radicals generated in the reaction of peroxy radicals with NO are produced with substantial internal vibrational excitation. Decomposition of vibrationally excited alkoxy radicals can occur on a time scale that is sufficiently short ($<10^{-10}$ s) to preclude collisional deactivation.

The decrease in COF_2 and increase in CH_3COF yields with increasing [NO] over the range 0−60 mTorr, seen in Figure 9, indicates a competition between reactions 5 and 28 for available CH_3CF_2O radicals. The fact that the COF_2 yield does not reach zero and the CH_3COF yield does not approach unity at high [NO] can be explained by the formation of vibrationally excited $CH_3CF_2O^*$ radicals which undergo prompt decomposition via reaction 27. Using the simple mechanism described above, we predicted the CH_3COF and COF_2 yields to depend on the NO concentration according to expression I:

$$Y_{CH_3C(O)F} = \frac{k_{15a}}{k_{15}}\left(\frac{(k_{28}/k_5)[NO]}{1 + (k_{28}/k_5)[NO]}\right) = 1 - Y_{COF_2} \quad (I)$$

where $Y_{CH_3C(O)F}$ and Y_{COF_2} are the molar yields of $CH_3C(O)F$ and COF_2, k_{15a}/k_{15} is the fraction of $CH_3CF_2O_2$ radicals which reacts with NO to give thermalized CH_3CF_2O radicals which then undergo either reaction 5 or 28, and k_{28}/k_5 is the rate constant ratio. The curves in Figure 9 show fits to the data. As seen from Figure 9, expression I provides a reasonable description of the observed dependence of the product yields on [NO]. The nonlinear least-squares fit to the COF_2 data gives $k_{15a}/k_{15} = 0.67 \pm 0.06$ and $k_{28}/k_5 = (4.14 \pm 1.42) \times 10^{-15}$ molecule^{-1} cm^3, and the fit to the CH_3COF data gives $k_{15a}/k_{15} = 0.69 \pm 0.07$ and $k_{28}/k_5 = (5.53 \pm 2.22) \times 10^{-15}$ molecule^{-1} cm^3. Within the admitted large uncertainties, consistent results were obtained from the two data sets. We choose to quote final values which are averages of the two determinations together with error limits which encompass the extreme of the ranges: $k_{15a}/k_{15} = 0.68 \pm 0.08$ and $k_{28}/k_5 = (4.8 \pm 2.9) \times 10^{-15}$ molecule^{-1} cm^3. By analogy with the existing database for alkoxy radicals,[15] the rate constant for reaction 28 is expected to be of the order of 10^{-11} cm^3 molecule^{-1} s^{-1}. Hence, we derive an estimate of $k_5 = 2 \times 10^3$ s^{-1}.

In addition to the products mentioned above, small residual IR product features were observed at 866, 1210, 1256, and 1766 cm^{-1}. There are four pieces of information that lead us to believe these features are attributable to CH_3CF_2ONO. First, the features scaled linearly in all experiments suggesting (but not proving) they are attributable to one compound. Second, the intensity of the features increased with [NO], consistent with their formation via the association reaction of CH_3CF_2O radicals and NO. Third, IR features at 1729 (N−O stretch), 1256 (CH_3 deformation), 1210 (CF_2 antisymmetric stretch), and 866 cm^{-1} (C−C skeletal stretch) are consistent with those expected from CH_3CF_2ONO. Fourth, when reaction mixtures were left to stand in the chamber in the dark, the unknown decayed (lifetime of approximately 2 h) to give CH_3COF. IR features attributable to the FNO expected coproduct were sought but not found. However, in light of the fact that FNO is lost rapidly (on a time scale of minutes), probably via reaction with the chamber walls,[30] it was not surprising that the FNO coproduct was not observed. Features attributable to CH_3CF_2ONO were calibrated from the observed formation of its decomposition product CH_3COF, and the sum of the CH_3CF_2ONO and CH_3COF yields are plotted in Figure 9. Finally, it should be noted that NO_2 is present in the system (albeit at levels typically much lower than those of NO) and will compete for CH_3CF_2O radicals. There was no discernible effect of initial NO concentration on the residual spectrum attributed to CH_3CF_2ONO, suggesting that reaction with NO_2 is not a major loss mechanism for CH_3CF_2O radicals in these experiments.

3.7. Mechanism of the OH + CH_3CHF_2 Reaction. To provide information concerning the mechanism of the reaction of OH radicals with CH_3CHF_2, mixtures of 150−400 mTorr of CH_3CHF_2, 50−100 mTorr of CH_3ONO, and 30−150 mTorr of O_2 in 700 Torr total pressure of N_2 diluent were subjected to UV radiation. As discussed in section 3.5, in the absence of excess NO, the CH_3CF_2 radicals formed in reaction channel 2a are converted into COF_2 in essentially 100% yield.

$$CH_3CHF_2 + OH \rightarrow CH_3CF_2 + H_2O \quad (2a)$$

$$\rightarrow CH_2CHF_2 + H_2O \quad (2b)$$

In contrast, reaction channel 2b will lead to the formation of an alkoxy radical which is expected to be converted into CF_2-HC(O)H.[15] The $[COF_2]/[CF_2HC(O)H]$ ratio following irradiation of $CH_3CHF_2/CH_3ONO/O_2/N_2$ mixtures provides a measurement of k_{2a}/k_{2b}. OH radicals react approximately 40 times more rapidly with $CF_2HC(O)H$ than with CH_3CHF_2.[11,31] To minimize loss of $CF_2HC(O)H$ via reaction with OH, experiments were performed using high concentrations and low consumptions (<1%) of CH_3CHF_2. The consumption of CH_3CHF_2 was inferred by the observed formation of its oxidation products.

Although COF_2 was observed as a product following irradiation of $CH_3CHF_2/CH_3ONO/NO/O_2/N_2$, there was no discernible formation of $CF_2HC(O)H$ and we are able to establish a lower limit of $k_{2a}/k_{2b} > 3$ from which we derive $k_{2a}/(k_{2a} + k_{2b}) > 0.75$ and $k_{2b}/(k_{2a} + k_{2b}) < 0.25$. The present work is the first direct study of the branching ratio for reaction 2. The result obtained herein can be compared to estimates based on kinetic arguments of $k_{2b}/(k_{2a} + k_{2b}) = 0.26$ by Kozlov et al.[8] and $k_{2b}/(k_{2a} + k_{2b}) < 0.10$ by Wilson et al.[9] An estimate of $k_{2b}/(k_{2a} + k_{2b})$ can also be made using Cl atom data for k_{1a} and k_{1b} from sections 3.2 and 3.3 and the correlation between Cl atom and OH radical reactivities given by the expression $\log(k(OH)) = (0.412 \pm 0.049) \times \log(k(Cl)) - (8.16 \pm 0.72)$.[32] Data from sections 3.2 and 3.3 give $k_{1a} = 2.52 \times 10^{-13}$ and $k_{1b} = 2.06 \times 10^{-15}$ from which we derive $k_{2a} = 4.46 \times 10^{-14}$ and $k_{2b} = 6.15 \times 10^{-15}$ and hence $k_{2a}/(k_{2a} + k_{2b}) = 0.88$ and $k_{2b}/(k_{2a} + k_{2b}) = 0.12$. The value of $k_2 = k_{2a} + k_{2b} = 5.1 \times 10^{-14}$ predicted from the Cl atom data is 40% greater than the value recommended by IUPAC.[11] This level of agreement between predicted and measured kinetic data can be considered to be satisfactory; systematic errors in the predicted k_{2a} and k_{2b} are likely to cancel in estimations of $k_{2a}/(k_{2a} + k_{2b}) = 0.88$ and $k_{2b}/(k_{2a} + k_{2b}) = 0.12$. Our experimental determination of $k_{2b}/(k_{2a} + k_{2b}) < 0.25$ is consistent with estimations based on the Cl atom kinetic data

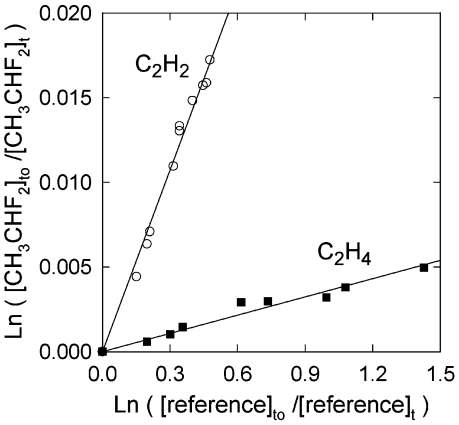

Figure 10. Loss of CH_3CHF_2 (inferred from COF_2 formation) vs C_2H_2 (open circles) and C_2H_4 (filled squares) following exposure to OH radicals in 700 Torr of air at 295 K.

in the present work and by Wilson et al.[9] but is slightly lower than that by Kozlov et al.[8]

3.8. Relative Rate Study of the Reaction of OH Radical with CH_3CHF_2. The kinetics of reaction 2 were measured relative to reactions 29 and 30.

$$CH_3CHF_2 + OH \rightarrow \text{products} \quad (2)$$

$$C_2H_4 + OH \rightarrow \text{products} \quad (29)$$

$$C_2H_2 + OH \rightarrow \text{products} \quad (30)$$

Initial concentrations were 110−120 mTorr of CH_3CHF_2, 150 mTorr of CH_3ONO, and 2−60 mTorr of either C_2H_4 or C_2H_2 in 700 Torr of air diluent. The loss of CH_3CHF_2 was measured indirectly from the observed formation of COF_2 by assuming OH-initiated oxidation of CH_3CHF_2 gives COF_2 in a molar yield of 0.875 ± 0.125 (value and range chosen to encompass the experimentally determined range $k_{2a}/(k_{2a} + k_{2b}) = 0.75-1.00$; see section 3.7). The loss of the reference gases was measured directly using FTIR spectroscopy. Figure 10 shows the loss of CH_3CHF_2 vs that of the reference compounds following exposure to OH radicals. Linear least-squares analysis of the data in Figure 10 gives $k_2/k_{29} = (3.59 \pm 0.27) \times 10^{-3}$ and $k_2/k_{30} = (3.58 \pm 0.12) \times 10^{-2}$. Using $k_{29} = 8.7 \times 10^{-12}$ [33] and $k_{30} = 8.45 \times 10^{-13}$,[34] we derive $k_2 = (3.12 \pm 0.23) \times 10^{-14}$ and $(3.03 \pm 0.10) \times 10^{-14}$ cm^3 molecule^{-1} s^{-1}. It is gratifying to note the agreement between the experiments conducted with the two different reference compounds. We estimate that potential systematic errors associated with uncertainties in the reference rate constants and COF_2 yield contribute additional 10 and 14% uncertainty ranges, respectively. Propagating these additional uncertainties gives $k_2 = (3.12 \pm 0.58) \times 10^{-14}$ and $(3.03 \pm 0.53) \times 10^{-14}$ cm^3 molecule^{-1} s^{-1}. We choose to cite a final value for k_2 which is the average of those determined using the two different reference compounds together with error limits which encompass the extremes of the individual determinations. Hence, $k_2 = (3.08 \pm 0.62) \times 10^{-14}$ cm^3 molecule^{-1} s^{-1}. The quoted uncertainty reflects the accuracy of the measurements. The value of k_2 determined in the present study is consistent with the IUPAC[11] and NASA-JPL[12] recommendations discussed in the Introduction.

4. Implications for Atmospheric Chemistry and the Environmental Impact of HFC-152a

We present a large body of self-consistent data concerning the atmospheric chemistry of CH_3CHF_2 (HFC-152a, R-152a). Cl atoms react with CH_3CHF_2 with a rate constant of $k_1 = (2.54 \pm 0.25) \times 10^{-13}$ cm^3 molecule^{-1} s^{-1}. The major (99.2%) reaction channel gives CH_3CF_2 radicals, and the minor (0.8%) channel gives CH_2CHF_2 radicals. Cl* atoms are lost rapidly in collisions with CH_3CHF_2 with a rate constant of $(2.21 \pm 0.22) \times 10^{-10}$ cm^3 molecule^{-1} s^{-1}, with the majority of loss occurring via collisional deactivation to give Cl atoms.

OH radicals react with CH_3CHF_2 with a rate constant of $k_2 = (3.08 \pm 0.62) \times 10^{-14}$ cm^3 molecule^{-1} s^{-1}. The major (>75%) reaction channel gives CH_3CF_2 radicals, and the minor (<25%) channel gives CH_2CHF_2 radicals. The atmospheric fate of CH_3CF_2 and CH_2CHF_2 radicals is the addition of O_2 to give peroxy radicals. Reaction of $CH_3CF_2O_2$ radicals with NO gives a substantial fraction of chemically activated alkoxy radicals, $[CH_3CF_2O]^*$. In 1 atm of air, approximately 30% of the alkoxy radicals produced in the $CH_3CF_2O_2$ + NO reaction possess sufficient internal excitation to undergo prompt (rate > 10^{10} s^{-1}) decomposition to give CH_3 radicals and COF_2. The remaining approximately 70% become thermalized, CH_3CF_2O, and undergo decomposition more slowly at a rate of approximately 2×10^3 s^{-1}. Reaction of $CHF_2CH_2O_2$ with NO gives CHF_2CH_2O radicals. The available database for fluorinated alkoxy radicals, although limited, indicates that the activation barrier for C−C bond scission is sufficiently large such that prompt decomposition of CHF_2CH_2O radicals will not be significant.[15] The atmospheric fate of CHF_2CH_2O radicals will be reaction with O_2 to give CHF_2CHO. CHF_2CHO has an atmospheric lifetime of approximately 1 week with respect to reaction with OH and photolysis which both lead to the formation of COF_2.[31] Irrespective of the site of attack, the reaction of the OH radical with HFC-152a will lead to the formation of COF_2. The atmospheric fate of COF_2 is incorporation into rain-, cloud-, and seawater followed by hydrolysis to give CO_2 and HF within a time frame of 1−2 weeks.[35] The additional fluoride ion burden associated with atmospheric oxidation of CH_3CHF_2 (HFC-152a) is of no environmental consequence.

In summary, the atmospheric lifetime of HFC-152a is determined by reaction with OH radicals and is approximately 1.4 years.[1] The bulk (>75%) of the atmospheric oxidation of HFC-152a generates COF_2 directly, and a minor fraction (<25%) generates COF_2 indirectly via $CHF_2C(O)H$. COF_2 is converted into CO_2 and HF within 1−2 weeks. The atmospheric oxidation products of HFC-152a are benign. HFC-152a does not contain chlorine and does not contribute to stratospheric ozone destruction. HFC-152a has a short atmospheric lifetime and will not contribute significantly to radiative forcing of climate change.

Acknowledgment. The Nagoya group thanks both Grants-in-Aid from the Ministry of Education, Culture, Sports, Science, and Technology, Japan, and the Steel Industrial Foundation for the Advancement of Environmental Protection Technology for financial support. M.P.S.A. thanks the Danish National Research Agency for a research grant. We thank Ole John Nielsen (Copenhagen University) for helpful comments.

References and Notes

(1) World Meteorological Organization. *Scientific Assessment of Ozone Depletion*; Report No. 47; Global Ozone Research and Monitoring Project: 2002.

(2) Tschuikow-Roux, E.; Yano, T.; Niedzielski, J. *J. Chem. Phys.* **1985**, *82*, 65.

(3) Yano, T.; Tschuikow-Roux, E. *J. Photochem.* **1986**, *32*, 25.

(4) Edney, E. O.; Driscoll, D. J. *Int. J. Chem. Kinet.* **1992**, *24*, 1067.

(5) Kaiser, E. W. *Int. J. Chem. Kinet.* **1993**, *25*, 667.

(6) Tuazon, E. C.; Atkinson, R. *J. Atmos. Chem.* **1993**, *17*, 179.
(7) Gierczak, T.; Talukdar, R.; Vaghjiani, G. L.; Lovejoy, E. R.; Ravishankara, A. R. *J. Geophys. Res.* **1991**, *96*, 5001.
(8) Kozlov, S. N.; Orkin, V. L.; Kurylo, M. J. *J. Phys. Chem. A* **2003**, *107*, 2239.
(9) Wilson, E. W., Jr.; Jacoby, A. M.; Kukta, S. J.; Gilbert, L. E.; DeMore, W. B. *J. Phys. Chem. A* **2003**, *107*, 9357.
(10) Nielsen, O. J. *Chem. Phys. Lett.* **1991**, *187*, 286.
(11) Atkinson, R.; Baulch, D. L.; Cox, R. A.; Crowley, J. N.; Hampson, R. W., Jr.; Kerr, J. A.; Rossi, M. J.; Troe, J. *Summary of Evaluated Kinetics and Photochemical Data for Atmospheric Chemistry*; IUPAC Subcommittee on Gas Kinetics Data Evaluation for Atmospheric Chemistry. http://www.iupac-kinetic.ch.cam.ac.uk/ (December 2002).
(12) Sander, S. P.; Friedl, R. R.; Golden, D. M.; Kurylo, M. J.; Huie, R. E.; Orkin, V. L.; Moortgat, G. K.; Ravishankara, A. R.; Kolb, C. E.; Molina, M. J.; Finlayson-Pitts, B. J. *Chemical Kinetics and Photochemical Data for use in Atmospheric Studies*; Evaluation No. 14; JPL Publication 02-25: 2003.
(13) Finlayson-Pitts, B. J.; Pitts, J. N., Jr. *Chemistry of the Upper and Lower Atmosphere, Theory, Experiments, and Applications*; Academic Press: New York, 2000.
(14) Tyndall, G. S.; Cox, R. A.; Granier, C. M.; Lesclaux, R.; Moortgat, G. K.; Pilling, M. J.; Ravishankara, A. R.; Wallington, T. J. *J. Geophys. Res.* **2001**, *106*, 12157.
(15) Orlando, J. J.; Tyndall, G. S.; Wallington, T. J. *Chem. Rev.* **2003**, *103*, 4657.
(16) Wallington, T. J.; Japar, S. M. *J. Atmos. Chem.* **1989**, *9*, 339.
(17) Matsumi, Y.; Tonokura, K.; Kawasaki, M. *J. Chem. Phys.* **1992**, *97*, 1065.
(18) Samartzis, P. C.; Bakker, B. L. G.; Rakitzis, T. P.; Parker, D. H.; Kitsopoulos, T. N. *J. Chem. Phys.* **1999**, *110*, 3351.
(19) Hitsuda, K.; Takahashi, K.; Matsumi, Y.; Wallington, T. J. *J. Phys. Chem. A* **2001**, *105*, 5131.
(20) Zhang, J.; Dulligan, M.; Wittig, C. *J. Chem. Phys.* **1997**, *107*, 1403.
(21) Hilbig, R.; Wallenstein, R. *IEEE J. Quantum Electron.* **1983**, *QE-19*, 1759.
(22) Chichinin, A. I. *J. Chem. Phys.* **2000**, *112*, 3772.
(23) Tyndall, G. S.; Orlando, J. J.; Kegley-Owen, C. S. *J. Chem. Soc., Faraday Trans.* **1995**, *91*, 3055.
(24) Wallington, T. J.; Hurley, M. D. *Chem. Phys. Lett.* **1992**, *189*, 437.
(25) Meagher, R. J.; McIntosh, M. E.; Hurley, M. D.; Wallington, T. J. *Int. J. Chem. Kinet.* **1997**, *29*, 619.
(26) Tyndall, G. S.; Orlando, J. J.; Kegley-Owen, C. S. *J. Chem. Soc., Faraday Trans.* **1995**, *91*, 3055.
(27) Matsumi, Y.; Izumi, K.; Skorokhodov, V.; Kawasaki, M.; Tanaka, N. *J. Phys. Chem. A* **1997**, *101*, 1216.
(28) Hitsuda, K.; Takahashi, K.; Matsumi, Y.; Wallington, T. J. *Chem. Phys. Lett.* **2001**, *346*, 16.
(29) Kim, Z. H.; Alexander, A. J.; Bechtel, H. A.; Zare, R. N. *J. Chem. Phys.* **2001**, *115*, 179.
(30) Wallington, T. J.; Schneider, W. F.; Szente, J. J.; Maricq, M. M.; Nielsen, O. J.; Sehested, J. *J. Phys. Chem.* **1995**, *99*, 984.
(31) Scollard, D. J.; Treacy, J. J.; Sidebottom, H. W.; Balestra-Garcia, C.; Laverdet, G.; LeBras, G.; MacLeod, H.; Téton, S. *J. Phys. Chem.* **1993**, *97*, 4684.
(32) Sulbaek Andersen, M. P.; Nielsen, O. J.; Wallington, T. J.; Hurley, M. D.; DeMore, W. B. *J. Phys. Chem. A* **2005**, *109*, 3926.
(33) Calvert, J. G.; Atkinson, R.; Kerr, J. A.; Madronich, S.; Moortgat, G. K.; Wallington, T. J.; Yarwood, G. *The mechanisms of atmospheric oxidation of the alkenes*; Oxford University Press: New York, 2000.
(34) Sørensen, M.; Kaiser, E. W.; Hurley, M. D.; Wallington, T. J.; Nielsen, O. J. *Int. J. Chem. Kinet.* **2003**, *35*, 191.
(35) Wallington, T. J.; Schneider, W. F.; Worsnop, D. R.; Nielsen, O. J.; Sehested, J.; DeBruyn, W.; Shorter, J. A. *Environ. Sci. Technol.* **1994**, *28*, 320A.